Article

Fluorinated metal phthalocyanines: interplay between fluorination degree, films orientation and ammonia sensing properties

Darya Klyamer [1], Aleksandr Sukhikh [1,2], Sergey Gromilov [1,2], Pavel Krasnov [3,4], Tamara Basova [1,2,*]

[1] Nikolaev Institute of Inorganic Chemistry SB RAS, Lavrentiev Pr. 3, Novosibirsk 630090, Russia
[2] Novosibirsk State University, Pirogova Str. 2, Russia
[3] Institute of Nanotechnology, Spectroscopy and Quantum Chemistry, Siberian Federal University, Krasnoyarsk, 660041, Russia
[4] Reshetnev Siberian State University of Science and Technology, 82 Mira prospect, Krasnoyarsk, 660049, Russia
* Correspondence: basova@niic.nsc.ru; Tel.: +7-383-330-8957

Received: date; Accepted: date; Published: date

Abstract: In this work, the sensor response of $MPcF_x$ (M=Cu, Co, Zn; x=0, 4, 16) films toward gaseous NH_3 (10-50 ppm) was studied by a chemiresistive method and compared to that of unsubstituted MPc films to reveal the effects of central metals and F-substituents on the sensing properties. A combination of atomic force microscopy and X-ray diffraction techniques has been used to elucidate the structural features of thin $MPcF_x$ films deposited by organic molecular beam deposition. It has been shown that the sensor response of $MPcF_4$ films to ammonia is noticeably higher than that of MPc films, which is in good correlation with the values of binding energy between the metal phthalocyanine and NH_3 molecule as calculated by DFT method. At the same time, in contrast to the DFT calculations $MPcF_{16}$ demonstrated the less sensor response compared to $MPcF_4$, which appeared to be connected with the different structure and morphology of their films. $ZnPcF_4$ films were shown to exhibit the sensitivity to ammonia up to the concentrations as low as 0.1 ppm and can be used for the selective detection of ammonia in the presence of some reducing gases and volatile organic compounds. Moreover, $ZnPcF_4$ films can be used for the detection of NH_3 in the gas mixture simulating exhaled air (N_2 – 76%, O_2 – 16%, H_2O – 5%, CO_2 – 3%).

Keywords: metal phthalocyanines; thin films; chemiresistive sensors; ammonia; DFT calculations

1. Introduction

Ammonia is an important commercial chemical used to make fertilizers, household cleaners, and refrigerants and to synthesize other chemicals. Despite of natural origin and wide distribution, ammonia is both highly toxic and corrosive gas in its concentrated form. It is classified as an extremely hazardous substance, and is subjected to strict monitoring of its concentration in environment, automotive and chemical industry [1]. The detected concentration levels of ammonia depend on application areas and can be varied in very wide range from ppb level to hundreds ppm [1].

Recently interest has been escalating into the study of exhaled breath as a noninvasive method of diagnostics for bronchopulmonary, cardiovascular, gastrointestinal and other diseases [2]. Inference can be made regarding changes in the metabolism and about the presence of a particular disease according to changes in the ratios of substances released in human breath. For example, ammonia concentration >1 ppm indicates renal failure in nephritis, atherosclerosis of the renal arteries, toxic affections of kidneys and other diseases [3].

There are several ammonia detection devices described in the literature. Among those, optical gas analyzers [4-6], catalytic ammonia sensors [1], metal-oxide gas sensors [7-8], conducting polymer

gas detectors [9-11] and chemiresistive sensors based on carbon nanomaterials and 2D transition metal dichalcogenides [12] are used for the detection of gaseous ammonia, with their virtues and shortcomings. Electrolytic devices usually suffer from their low detection limits and limited accuracy while optical sensors have very good sensitivity, but they are usually suited only for laboratory testing rather than for low cost portable sensors. Conducting polymer-based sensors generally suffer from irreversible sensor response and low selectivity in the presence of other gases [13].

Thin films of metal phthalocyanine (MPc) derivatives and their hybrid materials are of considerable interest as active layers of chemiresistive sensors for ammonia detection [14, 15]. Introduction of various substituents into the phthalocyanine macrocycle can significantly alter the films structure and morphology and in its turn leads to the change of their electrical and sensing properties [15-16]. Fluorine substituents decrease the electron density of the aromatic ring and increase the oxidation potential of the MPc molecule [17]. As a result, fluorosubstituted phthalocyanines exhibit higher sensor response to such reducing gases as ammonia and hydrogen [18]. The better sensor response of $ZnPcF_{16}$ and $PdPcF_{16}$ films towards gaseous ammonia compared to their unsubstituted analogues was presented by Schollhorn *et al.* [19-20] and Klyamer *et al.* [15], respectively. To the best of our knowledge, only sporadic data on structural features and sensing behavior of tetrafluorosubstituted metal phthalocyanine ($MPcF_4$) films are available in the literature [15-16, 21]. In our previous work [15], we studied the structure of $CoPcF_4$ films deposited by thermal evaporation and their sensor response to ammonia. It has been shown that similarly to the case of $MPcF_{16}$, the sensor response to ammonia is noticeably higher compared to unsubstituted CoPc films. To the best of our knowledge, the systematic analysis of the interplay between fluorination degree, films orientation and sensing properties have never been carried out in the literature.

In this work, the sensor response of $MPcF_x$ (M=Cu, Co, Zn; x=4, 16) films toward gaseous NH_3 (10-50 ppm) was studied by chemiresistive method and compared to that of unsubstituted MPc films to reveal the effects of central metals and F-substituents on the sensing properties. A combination of atomic force microscopy and X-ray diffraction techniques has been used to elucidate the structural features and molecular orientation of thin films of $MPcF_x$ deposited by organic molecular beam deposition. DFT calculations have been performed to estimate the probable structure of $MPcF_x$-analyte complexes and their bond formation energies. Sensor characteristics of $ZnPcF_4$ films were studied in more details to demonstrate their application for selective detection of low concentration of ammonia (up to 0.1 ppm) in the presence of CO_2 and water vapors as well as in the gas mixture with the composition close to exhaled air (N_2 – 76%, O_2 – 16%, H_2O – 5%, CO_2 – 3%).

2. Materials and Methods

2.1. Preparation and study of thin films

Unsubstituted (MPc, M=Cu, Co, Zn), tetrafluorosubstituted ($MPcF_4$, M=Cu, Co, Zn) and hexadecafluorosubstituted ($MPcF_{16}$, M=Cu, Co, Zn) phthalocyanines were synthesized according to the procedures described elsewhere [15, 16] from the corresponding phthalonitrile derivatives and corresponding metal chlorides. $MPcF_4$ derivatives were prepared as a statistical mixture of four regioisomers due to the various possible positions of fluorine substituents. The isomers were not separated because of close parameters of sublimation.

Thin films of all investigated phthalocyanines were deposited by organic molecular beam deposition under vacuum of 10^{-5} Torr onto platinum interdigitated electrodes (Dropsens, Spain). The electrodes have the following dimensions: gap between digits is 10 μm; number of digits is 125x2 with a digit length of 6760 μm; cell constant is 0.0118 cm^{-1}. The nominal thickness of phthalocyanine films was about 100 nm.

XRD studies of thin film samples were carried out using a Shimadzu XRD-7000 diffractometer (CuKα, λ=1.54187Å, Bragg-Brentano scheme, θ-θ goniometer, copper anode sealed tube 30mA@40kV with a Ni filter and scintillation counter detector). Scan range was from 5° to 30° 2θ, with the step of 0.03° and the acquisition time of 40s per step. AFM in tapping mode with a

Nanoscope IIIa (Veeco Instruments, Plainview, U.S.A.) scanning probe microscope was used for the characterization of the films morphology.

To test the chemiresistive sensor response the films were put into the flow cell and held for 10 min under air flow until the resistance reached a steady state value. Then NH_3 gas (0.1-50 ppm) was diluted with air and injected. Air was used as the dilution and carrier gas. The electrical resistance of phthalocyanine films was measured with a Keithley 236 electrometer by applying a constant dc voltage (8 V). All gas sensing measurements were carried out at room temperature.

2.2. Theoretical calculations

Interaction of MPc, $MPcF_4$ and $MPcF_{16}$ with NH_3 was studied by the density functional theory (DFT) using the BP86/def2-SVP method [22-25] and Grimme D3 dispersion correction [26, 27]. The ORCA suite of quantum chemical programs was used for all calculations [28].

The binding energy (E_b) was calculated according to the Equation (1) as a difference of the total energies of the corresponding adduct and its interacting components:

$$E_b = E_{\mathrm{CoPcF_x\text{-}NH_3}} - E_{\mathrm{NH_3}} - E_{\mathrm{CoPcF_x}} \quad (1)$$

The effective charge $q(NH_3)$ was calculated according to the Equation (2)

$$q = \sum_n \left(Z_n - \sum_{I \in n} \sum_J P_{IJ} S_{IJ} \right), \quad (2)$$

where Z_n is the nuclear charge of the atom n; P_{IJ} and S_{IJ} are the elements of the density and overlap matrixes corresponding to the atomic orbitals I and J. This scheme realized in ORCA is based on the widely used Mulliken population analysis [29, 30]. A bond order was estimated using Mayer's method [31, 32].

3. Results and Discussion

3.1. Experimental study of the dependence of sensing response on phthalocyanine molecular structure

The sensor response of $MPcF_x$ (M=Cu, Co, Zn; x=4, 16) films was studied by a chemiresistive method. The choice of phthalocyanines of copper, cobalt and zinc was determined by their better sensitivity to ammonia according to the experimental data and DFT calculations performed earlier by Liang *et al.* [33]. The change of the film resistance during the sequential injection of the gas analyte and air purging was measured. The typical sensor response toward ammonia is shown in Figure 1 using $CoPcF_4$ and $CoPcF_{16}$ (b) films as an example.

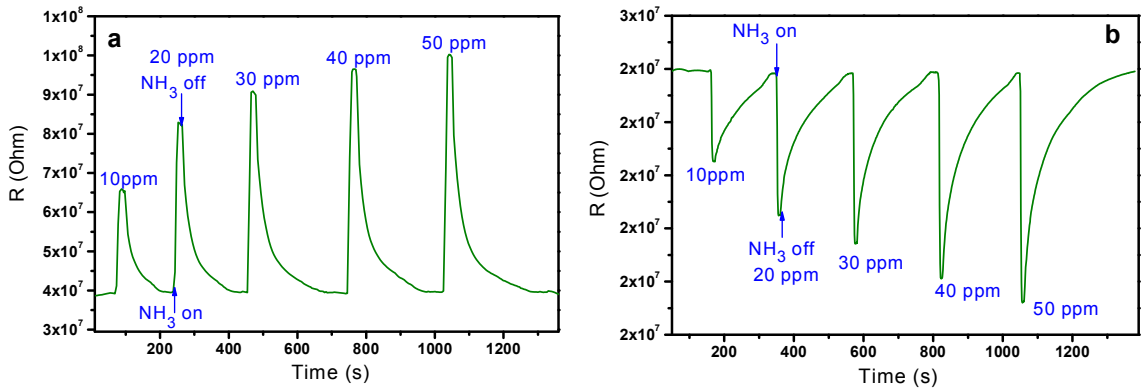

Figure 1. Sensor response of $CoPcF_4$ (a) and $CoPcF_{16}$ films (b) to ammonia (10-50 ppm).

Introduction of ammonia to the gas cell leads to the increase of resistance of CoPc and $CoPcF_4$ films. Similar behavior typical for organic semiconductor films possessing p-type conductivity [34] was also observed in the case of ZnPc, CuPc, $ZnPcF_4$ and $CuPcF_4$ films.

The resistance-based sensing mechanism of semiconducting sensors has been studied in the literature [35, 36]. It has been reported that the formation of charge-transfer complexes by coordination of O_2 to MPc at the air/phthalocyanine interface and at grain boundaries leads to the formation of oxidized MPc^+ and O^{2-} species and injection of hole charge carriers into the film's bulk [37, 38]. When a p-type semiconductor gas sensor is exposed to the reducing NH_3 gas, the electrons injected into the material through the oxidation reaction between the reducing gas and the O^{2-} species on the semiconductor surface decrease the concentration of holes in the layer, which in turn increases the resistance of MPc film [39].

On the contrary, $MPcF_{16}$ (M=Co, Cu, Zn) films exhibit a decrease of their resistance upon interaction with electron donor NH_3 molecules. It is known that perfluorinated metal phthalocyanines demonstrate the n-conducting behavior due to the effect of electron-withdrawing fluorine substituents [40, 41]. When an n-type semiconductor gas sensor is exposed to the reducing NH_3 gas, ionized oxygen anions are used to oxidize the reducing gas, and the released electrons inject into the semiconducting core, which decreases the sensor resistance proportionally to the concentration of reducing gas-analyte [36].

To study the influence of phthalocyanine molecular structure on the sensing behavior the sensor responses of $MPcF_x$ (M=Co, Cu, Zn; n=0, 4, 16) films toward ammonia were compared in the concentration range from 10 to 50 ppm. Figure 2 shows the dependence of the relative sensor response $R_n=|R-R_o|/R_o$ (where R is the resistance at a certain concentration of the analyte, R_o is the resistance before injection of the analyte vapors) for MPc, $MPcF_4$ and $MPcF_{16}$ films. It can be seen that the sensor response decreases in the order $CoPcF_x > ZnPcF_x > CuPcF_x$ both in the case of unsubstituted (Figure 2a) and fluorinated derivatives (Figure 2b,c). For instance, the sensor response of CoPc films toward 10 ppm of ammonia is about 2 times higher compared to ZnPc films and 8 times higher compared to CuPc films (Figure 2a). Even more pronounced difference is observed in the case of $MPcF_4$ and $MPcF_{16}$ films, e.g. the sensor response of $CoPcF_x$ (x=4, 8) films toward 10 ppm of ammonia is about 4 times higher compared to $ZnPcF_x$ films and 13 times higher compared to $CuPcF_x$ films (Figure 2b,c).

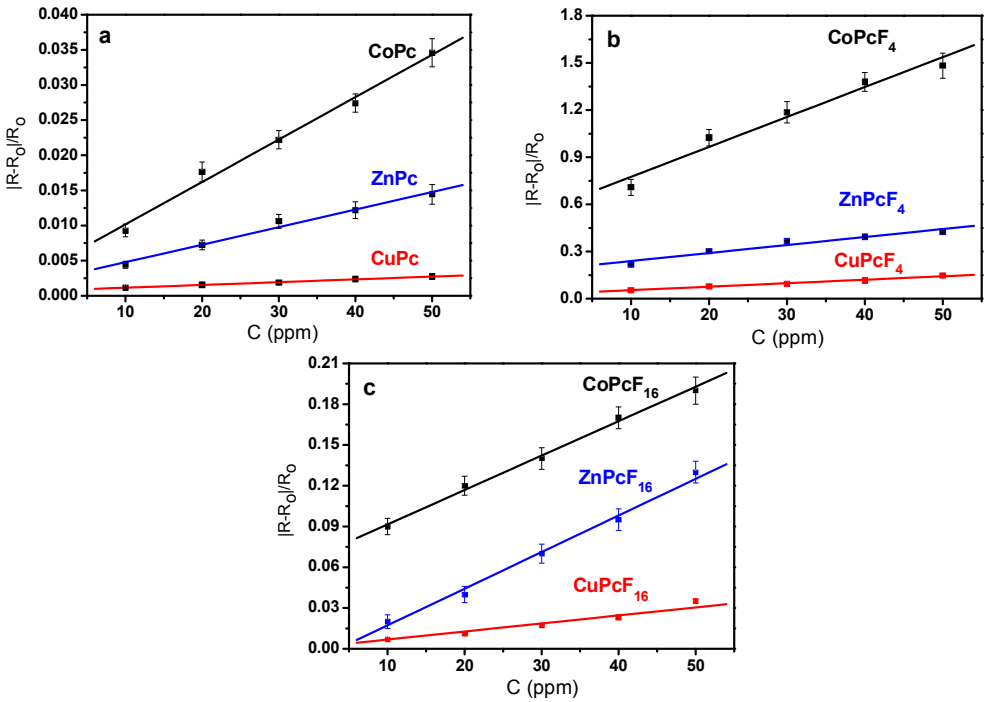

Figure 2. Dependence of the relative sensor response $|R-R_o|/R_o$ on NH_3 concentration (10-50 ppm) for MPc (a), $MPcF_4$ (b), $MPcF_{16}$ (c) (M= Zn, Co, Cu) films.

Figure 3 demonstrates the effect of F-substitution in phthalocyanine ring on the sensing response to ammonia using $ZnPcF_x$ (x=0, 4, 16) films as an example. The sensor response decreases in the order $ZnPcF_4 > ZnPcF_{16} > ZnPc$. The same order is also observed for $CuPcF_x$ and $CoPcF_x$ films.

$MPcF_4$ films exhibit the maximal sensor response to ammonia among all investigated phthalocyanines, e.g. the sensor response of $MPcF_4$ (M=Zn, Co, Cu) films is 3-10 times higher than that of $MPcF_{16}$ films and 30-70 times higher than that of MPc films. Therefore the introduction of F-substituents to the phthalocyanine macrocycle leads to a substantial increase of their sensitivity to ammonia.

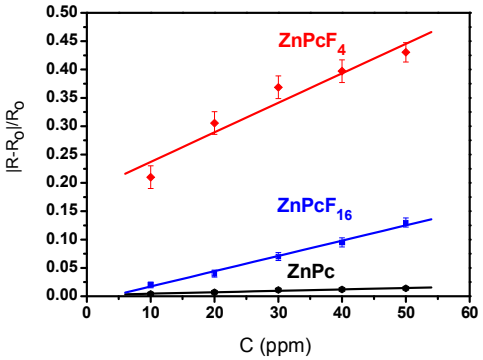

Figure 3. Dependence of the sensor response $|R-R_o|/R_o$ on NH_3 concentration (10-50 ppm) for ZnPc, $ZnPcF_{16}$ and $ZnPcF_4$ films.

The plots of dependencies of the response and recovery times on NH_3 concentration (10-50 ppm) for $ZnPcF_x$ (a), $CoPcF_x$ (b), $CuPcF_x$ (c) (x=0, 4, 16) films are shown in Figure 4. The average values of response and recovery times of all investigated films are also given in Table 1. All investigated films exhibited a reversible sensor response at room temperature with the response time of 10-25 s. The maximal recovery times are observed in the case of $CoPcF_x$ films and decrease in the order $CoPcF_x$ > $ZnPcF_x$ > $CuPcF_x$. This order correlates with the energy of binding of $MPcF_x$ with analyte molecules as shown below in the Section 3.2. The more binding energy between $MPcF_x$ and NH_3 the higher value of recovery time is observed.

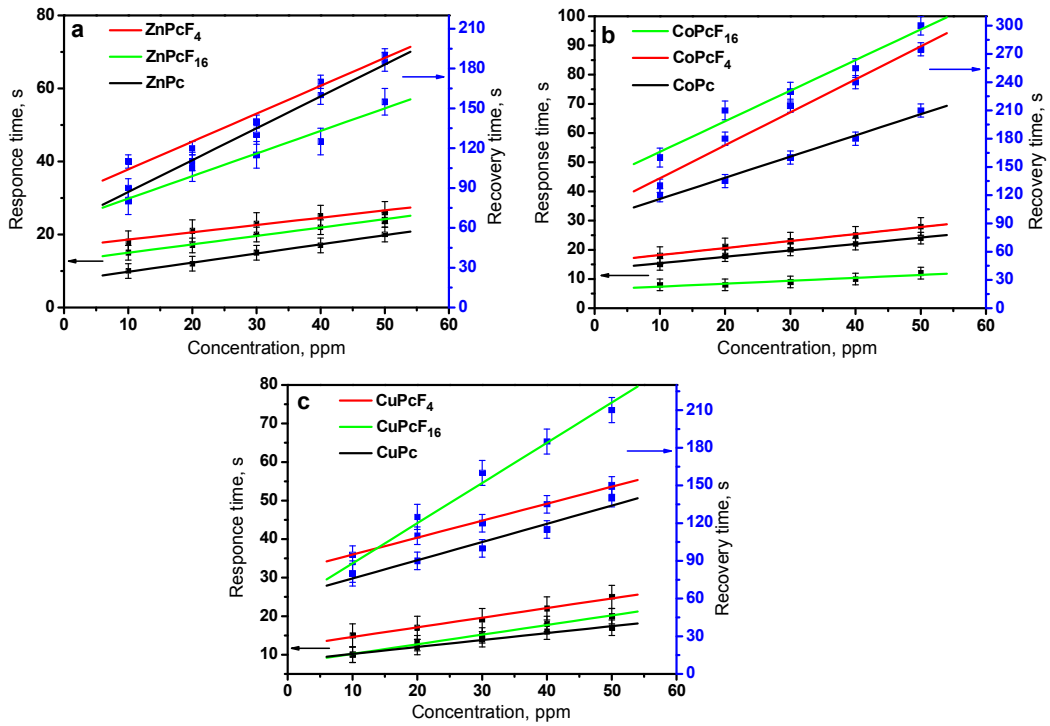

Figure 4. Dependence of the response and recovery times on NH_3 concentration (10-50 ppm) for $ZnPcF_x$ (a), $CoPcF_x$ (b), $CuPcF_x$ (c) (x=0, 4, 16) films.

Table 1. Average values of response and recovery times of MPc, $MPcF_4$, and $MPcF_{16}$ films at the concentration of ammonia 10 ppm.

Time, s	CoPc	$CoPcF_4$	$CoPcF_{16}$	ZnPc	$ZnPcF_4$	$ZnPcF_{16}$	CuPc	$CuPcF_4$	$CuPcF_{16}$
Response	15	20	10	10	25	15	10	15	10
Recovery	120	130	160	90	110	85	80	95	80

Sensor response of the sensing layers depends on several factors, among them the molecular structure of sensing material which governs the nature and strength of its interaction with an analyte and the sensing layer structure and morphology which determines the number of active sites and the rate of adsorption-desorption process.

3.2. Theoretical study of the dependence of sensor response on the phthalocyanine molecular structure

DFT calculations have been performed to study the interaction of NH_3 molecules with $MPcF_x$ and to elucidate the different sensor response of $MPcF_x$ with different x and central metals. To check the validity of theoretical model, the calculated vibrational spectra of $MPcF_x$ were compared with the experimental ones as has already been described elsewhere [15].

The most favorable structure of MPc····NH_3 aggregates simulated by DFT calculations was that with NH_3 molecule binding with phthalocyanine via its central metal. The binding of $MPcF_x$ with NH_3 molecule increases the out-of-plane distortion of the Pc ring, e.g. the out-of-plane displacement of the Zn atom in $ZnPcF_4$ leads to an increase in the Zn-N_α bond length from 2.007 Å to 2.043 Å in average. The binding parameters for NH_3 with $MPcF_x$ are presented in Table 2 for comparison. It has already been shown elsewhere [15, 42] that ammonia and MPcs form complexes with charge transfer from NH_3 to phthalocyanine molecule via interaction of NH_3 with the central metal ion inside the phthalocyanine macrocycle.

The formation of this bond is based on the displacement of electron density from NH_3 molecule to MPc through the central metal atom and as a result NH_3 acquires a positive effective charge increasing in the order CuPc<ZnPc<CoPc both for unsubstituted and fluorinated derivatives (Table 2). At the same time, the M-NH_3 bond order increases, and the respective distance d between the metal atom and ammonia nitrogen atom decreases in the same order. The obtained theoretical data are in a good correlation with the experimental investigations of sensor response of MPc (M=Cu, Zn, Co) which is higher in the case of cobalt phthalocyanines.

Table 2. Parameters of binding of NH_3 with MPc, $MPcF_4$ and $MPcF_{16}$

Aggregate	E_b, eV	Bond order	d, Å	$q(NH_3)$, e
CoPc····NH_3	-1.14	0.484	2.153	0.243
$CoPcF_4$····NH_3	-1.16	0.486	2.152	0.245
$CoPcF_{16}$····NH_3	-1.20	0.491	2.151	0.250
ZnPc····NH_3	-1.06	0.402	2.159	0.214
$ZnPcF_4$····NH_3	-1.08	0.405	2.156	0.216
$ZnPcF_{16}$····NH_3	-1.14	0.414	2.151	0.223
CuPc····NH_3	-0.62	0.291	2.330	0.156
$CuPcF_4$····NH_3	-0.63	0.293	2.329	0.158
$CuPcF_{16}$····NH_3	-0.68	0.302	2.322	0.164

As for the effect of F-substituents, the binding energy between NH_3 and $MPcF_x$ and the positive effective charge of NH_3 increase in the order MPc····NH_3<$MPcF_4$····NH_3<$MPcF_{16}$····NH_3 (Table 2). The experimental investigations of the sensor response of unsubstituted and fluorinated phthalocyanines showed that its value is higher in the case of $MPcF_4$. However it is necessary to mention that in contrast to the theoretical calculations the experimental sensor response of $MPcF_4$

films is higher than that of $MPcF_{16}$ films. It is conceivable that such behavior can be associated with different semiconductor properties and mechanisms of conductivity of $MPcF_4$ and $MPcF_{16}$ films. It has already been mentioned above that $MPcF_4$ films possess p-type conductivity, whereas $MPcF_{16}$ films demonstrate the *n*-conducting behavior. One more important factor governing the sensing properties is the structure and morphology of sensing layers.

3.3. Characterization of thin films

To study the effect of fluorination the structure and morphology of $MPcF_x$ films were investigated by XRD and AFM methods. X-ray diffraction patterns of thin films of all 9 phthalocyanine derivatives are shown in Figure 5. The diffraction patterns contain a single strong diffraction peak in the range from 5 to 7° 2θ and several barely visible peaks with the corresponding interplanar distances *d* which are the natural fractions of the d_0 of the strong peak. This type of diffraction patterns is a typical feature of thin films with a strong preferred orientation. Comparing the interplanar distances with the calculated ones known from the single crystal data [43, 44], CoPc and CuPc thin films were identified as metastable α-polymorphs. There are no known structural data for α-ZnPc, however, some works show that α-ZnPc is isostructural to α-CuPc and α-CoPc and it forms when deposited onto the substrate surface at temperatures lower than 100 °C [45].

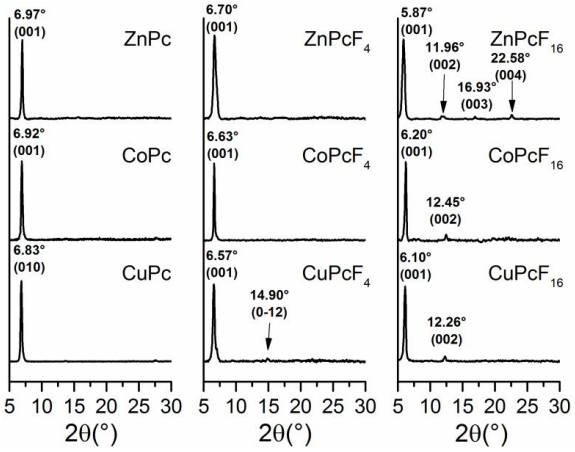

Figure 5. XRD patterns for thin film samples of $MPcF_x$ (M=Zn, Co, Cu; x=0, 4, 16).

$CuPcF_4$, $CoPcF_4$ and $ZnPcF_4$ are isostructural with $PdPcF_4$ [16] and crystallize only in one triclinic (P-1 space group) phase. There are two known polymorphs for $CuPcF_{16}$, *viz.* α-$CuPcF_{16}$ (P-1 space group, Z=1) [46] and triclinic β-$CuPcF_{16}$ (P-1 space group, Z=2) [47] and both of them have very similar values of interplanar distances for the first peak on the calculated diffraction pattern. α-$CuPcF_{16}$ grows on the substrate surface at room temperature, while β-$CuPcF_{16}$ are obtained at 360 °C. Since in this work the substrate temperature was about 20 °C, it is reasonable to assume that $CuPcF_{16}$ thin film consists of α-phase. No crystal structure data are known for α-polymorphs of $CoPcF_{16}$ and $ZnPcF_{16}$, but since α-CuPc/α-CoPc, $CuPcF_4$/$CoPcF_4$/$ZnPcF_4$ and β-$CuPcF_{16}$/β-$CoPcF_{16}$/β-$ZnPcF_{16}$ are isostructural to each other, we assumed that $CoPcF_{16}$ and $ZnPcF_{16}$ thin films are also α-polymorphs with the same structure as α-$CuPcF_{16}$.

Figure 6 shows AFM images of the surface of ZnPc (a), $ZnPcF_4$ (b) and $ZnPcF_{16}$ (c) films. As can be clearly seen that the ZnPc film surface consists of roundish grains (Figure 6a) and has the rms roughness value of 14.2 nm. The $ZnPcF_4$ film having an rms roughness of 6.7 nm is formed by azimuthally disordered elongated grains (Figure 6b). $ZnPcF_{16}$ films exhibit a high density of azimuthally disordered roundish grains with the size noticeably smaller than those of ZnPc films and the minimal rms roughness values (4.2 nm) among the investigated films (Figure 6c). More rough and inhomogeneous surface of $ZnPcF_4$ films can also be responsible for their higher sensor response to ammonia compared to $ZnPcF_{16}$ films.

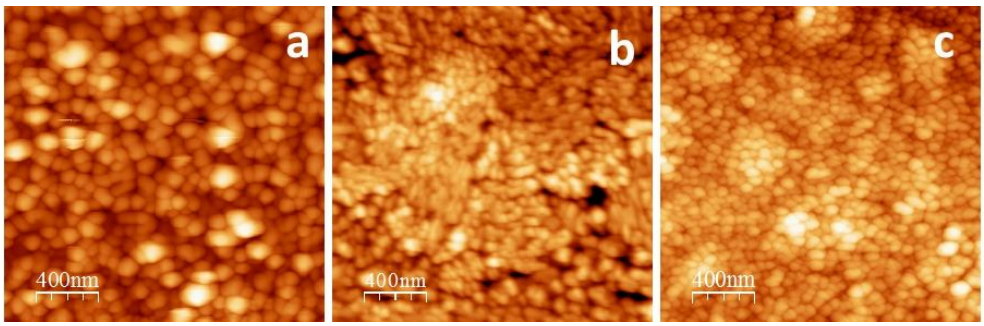

Figure 6. AFM images of ZnPc (a), $ZnPcF_4$ (b) and $ZnPcF_{16}$ (c) films.

3.4. Sensor characteristics of phthalocyanine films

Sensor characteristics of $MPcF_4$ films demonstrating the best sensitivity to ammonia among the investigated samples were studied in more details to demonstrate their applicability for the detection of NH_3 at lower concentrations down to 0.1 ppm in the presence of other gases. A typical sensor response of a $ZnPcF_4$ layer toward ammonia in the concentration range from 1-4 ppm is shown in Figure 7a. To demonstrate possible application of $ZnPcF_4$ films for detection of gases-biomarkers in exhaled air, the sensor response of $ZnPcF_4$ films to ammonia was also tested in a mixture of gases with the composition close to exhaled air of healthy people. For this purpose, small amounts of ammonia (1-4 v.%) were added to the preliminarily prepared gas mixture (N_2 – 76%, O_2 – 16%, H_2O – 5%, CO_2 – 3%). The sensor response of a $ZnPcF_4$ film to ammonia (1-4 ppm) diluted with the mixture of gases N_2 – 76%, O_2 – 16%, H_2O – 5%, CO_2 – 3% is shown in Figure 7b.

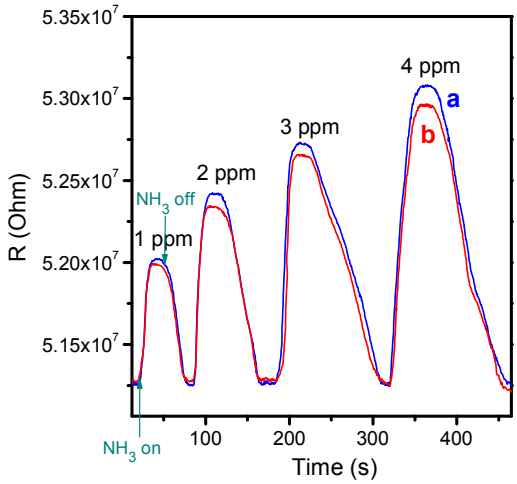

Figure 7. Sensor response of a $ZnPcF_4$ layer toward ammonia in the concentration range from 1 to 4 ppm, in air (a) and in a mixture of gases with the composition close to exhaled air of healthy people (N_2 – 76%, O_2 – 16%, H_2O – 5%, CO_2 – 3%) (b).

$ZnPcF_4$ films demonstrate reversible sensor response in the investigated concentration range with a quite good response and recovery time; the response time varied from 15 s to 30 s depending on NH_3 concentration, while the recovery time increased from 28 s to 90 s when NH_3 concentration changes from 1 to 4 ppm. The dependence of sensor response on NH_3 concentration is given in Figure 8. The minimum detected concentration of NH_3 in the case of $ZnPcF_4$ films was found to be 0.1 ppm.

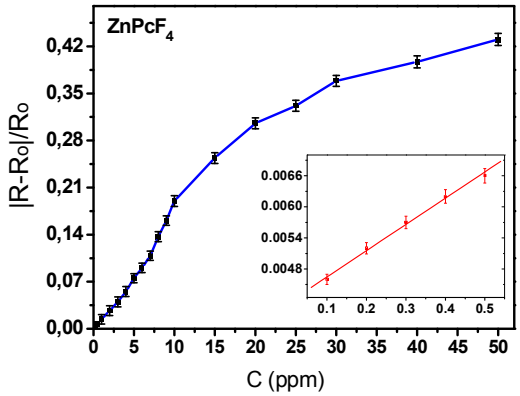

Figure 8. Dependence of the sensor response of $ZnPcF_4$ film on NH_3 concentration (0.1-50 ppm).

To study the selectivity of $ZnPcF_4$-based sensors their response was tested against ammonia (10 ppm), acetone (1000 ppm), dichloromethane (10^4 ppm), carbon dioxide (10^4 ppm) and ethanol (10^4 ppm). Figure 9a shows that the sensor exhibited a significantly higher response to ammonia in comparison with that toward the other investigated analytes. This obviously indicates the viability of this type of sensors to detect ammonia selectively in the presence of other gases such as those tested in this work. Note that the investigated interfering gases were taken at much higher concentration compared to ammonia.

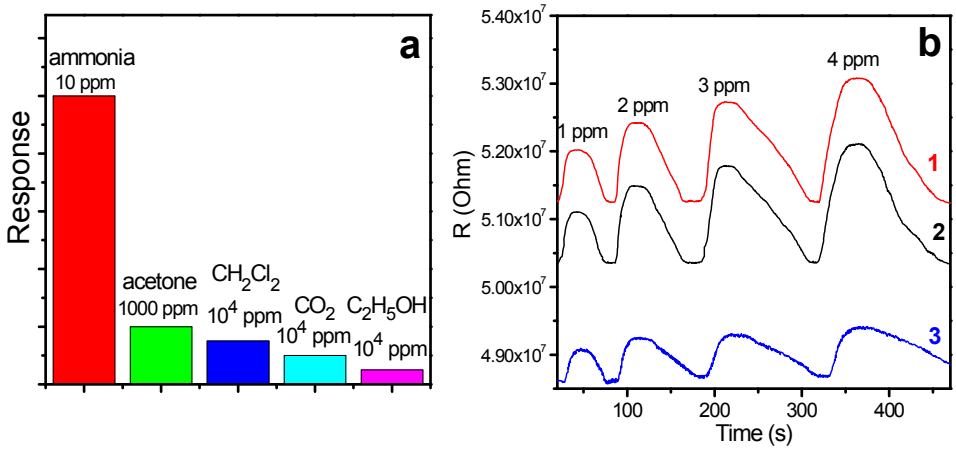

Figure 9. (a) - Response of a $ZnPcF_4$ film to ammonia (10 ppm), acetone (1000 ppm), dichloromethane (10^4 ppm), carbon dioxide (10^4 ppm), ethanol (10^4 ppm). (b) - Response of a $ZnPcF_4$ film to ammonia (1-4 ppm) in air measured at relative humidity 5% (1), 30% (2) and 70% (3).

The dependence of the sensor response on relative humidity (RH) was also examined and the results are presented in Figure 9b, which show that the initial resistance of $ZnPcF_4$ film decreases with the increase of RH from 5% to 70%. The value of sensor response to NH_3 at RH 5% and 30% is almost the same, however, it is found to decrease noticeably with increasing RH to 70%. The main reason of such behavior appears to be a competitive sorption of NH_3 and H_2O molecules on the surface of the $ZnPcF_4$ film.

The sensor response of a $ZnPcF_4$ layer toward ammonia in air was also compared with that in a mixture of gases with the composition close to exhaled air of healthy people. Figures 7b shows that the value of sensor response to NH_3 in the presence of gas mixture (N_2 – 76%, O_2 – 16%, H_2O – 5%, CO_2 – 3%) is almost the same as in the mixture with air. This makes $ZnPcF_4$ films a promising sensing layer for the detection of ammonia in exhaled air, which is used as a gas-biomarker of renal failure in nephritis, atherosclerosis of the renal arteries and toxic affections of kidneys [3].

Note that the sensor performance of several sensors towards ammonia has been reported in the literature [48-54]. Some examples of sensor characteristics of several sensors including the data obtained in this work are summarized in Table 3 for comparison.

Table 3. Sensor performance of active layers based on metal oxides, conducting polymers, carbon-containing nanomaterials and phthalocyanines

Sensing layer	Concentration range, ppm	Minimal investigated concentration, ppm	Response/ recovery time, s	Temperature range, °C	Ref.
Metal oxides					
Pt/NiO	1-1000	0.01	15/76 (350°C, 1000 ppm)	200-350	[7]
Pt Nanoparticle/ Aluminum-Doped Zinc Oxide	1-1000	1	24/4 (350 °C, 1000 ppm)	200-350	[48]
Conducting polymers					
Polyaniline/poly(styrene-butadiene-styrene)	0.1-100	0.1	≤13 (100 ppm)/--	Room temperature	[49]
Flexible polyaniline films	50-150	50	40 (50 ppm)/--	Room temperature	[50]
Carbon-containing nanomaterials and phthalocyanines					
AuNPs /SWNT	0.25-6	0.255	20 (0.4 ppm)/--	Room temperature	[51]
rGO modified with metal tetra-α-iso-pentyloxyme-tallophthalocyanines (CuPc, NiPc, PbPc)	0.4-400	0.4	CuPc/rGO 364/115 NiPc/rGO 200/264 PbPc/rGO 248/331 (0.8 ppm)	Room temperature	[52]
CoPc on a flexible polyethylene terephthalate substrate	5-50	5	25/156 (20 ppm)	Room temperature	[53]
$ZnPcF_4$	0.1-50	0.1	25/110 (10 ppm)	Room temperature	This work

The sensing layers based on $ZnPcF_4$ are quite competitive with the active layers based on metal oxides, conducting polymers and carbon-containing nanomaterials, described in the literature; $ZnPcF_4$ film exhibit reversible sensor response at room temperature, low detection limit, as well as low values of response and recovery times compared to the other sensors.

Conclusions

In this work, unsubstituted metal phthalocyanines (MPc, M=Cu, Co, Zn), tetrafluorosubstituted metal phthalocyanines ($MPcF_4$) and hexadecafluorosubstituted metal phthalocyanines ($MPcF_{16}$) thin films were deposited by organic molecular beam deposition and studied to reveal the effects of the central metals and F-substituents on the films sensor response to ammonia.

It has been shown that the sensor response decreased in the order $CoPcF_x > ZnPcF_x > CuPcF_x$ both in the case of unsubstituted and fluorinated derivatives. The sensor response of $MPcF_4$ films to ammonia is noticeably higher than that of MPc films, which is in good correlation with the values of binding energy between the metal phthalocyanine and NH_3 molecule as calculated by DFT method. At the same time, in contrast to the DFT calculations $MPcF_{16}$ demonstrated the less sensor response compared to $MPcF_4$, which appeared to be connected with the different structure and morphology of their films.

It has been shown using $ZnPcF_4$ films as an example that they exhibit the sensitivity to ammonia up to the concentrations as low as 0.1 ppm and can be used for the selective detection of ammonia in the presence of some reducing gases and volatile organic compounds. Moreover, $ZnPcF_4$ films can be used for the detection of NH_3 in the gas mixture simulating exhaled air (N_2 – 76%, O_2 – 16%, H_2O – 5%, CO_2 – 3%). This makes these films promising active layers as chemiresistive sensors for the detection of ammonia in exhaled air, which is a biomarker of some kidney diseases.

Author Contributions: Conceptualization, T.B.; Methodology, P.K.; Validation, D.K., A.S., S.G and T.B.; Formal Analysis, A.S.; Investigation, D.K. and A.S.; Writing-Original Draft Preparation, D.K. and T.B.; Writing-Review & Editing, T.B.; Visualization, A.S.; Supervision, S.G.; Project Administration, T.B.; Funding Acquisition, T.B.

Funding: This research was funded by FASO of Russian Federation (project 0300-2016-0007).

Acknowledgments: The authors are grateful to the Data-Computing Center of Novosibirsk State University for the provision supercomputer facility.

Conflicts of Interest: The authors declare no conflict of interest. The funders had no role in the design of the study; in the collection, analyses, or interpretation of data; in the writing of the manuscript, and in the decision to publish the results.

References

1. Timmer, B.; Olthuis, W.; van den Berg, A. Ammonia sensors and their applications: A review. *Sens. Actuators B* **2005**, *107*, 666–677, 10.1016/j.snb.2004.11.054.
2. Di Natale, C.; Paolesse, R.; Martinelli, E.; Capuano, R. Solid-state gas sensors for breath analysis: A review. *Anal. Chim. Acta* **2014**, *824*, 1–17, 10.1016/j.aca.2014.03.014.
3. DuBois, S.; Eng, S.; Bhattacharya, R.; Rulyak, S.; Hubbard, T.; Putnam, D.; Kearney, D. Breath Ammonia Testing for Diagnosis of Hepatic Encephalopathy. *Digestive Diseases Sci.* **2005**, *50*, 1780–1784, 10.1007/s10620-005-2937-6.
4. Mount, G.H.; Rumberg, B.; Havig, J.; Lamb, B.; Westberg, H.; Yonge, D.; Johson, K.; Kincaid, R. Measurement of atmospheric ammonia at a dairy using differential optical absorption spectroscopy in the mid-ultraviolet. *Atmos. Environ.* **2002**, *36*, 1799–1810, 10.1016/S1352-2310(02)00158-9.
5. Jin, Z.; Su, Y.; Duan, Y. Development of a polyaniline-based optical ammonia sensor. *Sens. Actuators B* **2001**, *72*, 75–79, 10.1016/S0925-4005(00)00636-5.
6. Lee, Y-S.; Joo, B-S.; Choi, N-J.; Lim, J-O.; Huh, J-S.; Lee, D-D. Visible optical sensing of ammonia based on polyaniline film. *Sens. Actuators B* **2003**, *93*, 148–152, 10.1016/S0925-4005(03)00207-7.
7. Chen, H.-I.; Hsiao, C-Y.; Chen, W.-C.; Chang, C.-H.; Chou, T.-C.; Liu, I.-P.; Lin, K.-W.; Liu, W.-C. Characteristics of a Pt/NiO thin film-based ammonia gas sensor. *Sens. Actuators B* **2018**, *256*, 962–967, 10.1016/j.snb.2017.10.032.
8. Joshi, N.; Hayasaka, T.; Liu, Y.; Liu, H.; Oliveira, O.N. Jr; Lin L. A review on chemiresistive room temperature gas sensors based on metal oxide nanostructures, graphene and 2D transition metal dichalcogenides. *Microchim. Acta* **2018**, *185*, 213, 10.1007/s00604-018-2750-5.
9. Kumar, L.; Rawal, I.; Kaur, A.; Annapoorni, S. Flexible room temperature ammonia sensor based on polyaniline, *Sens. Actuators B* **2017**, *240*, 408–416, 10.1016/j.snb.2016.08.173.
10. Park, S.J.; Park, C.S., Yoon, H. Chemo-Electrical Gas Sensors Based on Conducting Polymer Hybrids. *Polymers* **2017**, *9*, 155, 10.3390/polym9050155.
11. Wang, Q.; Wu, S.; Ge, F.; Zhang, G.; Lu, H.; Qiu, L. Solution-Processed Microporous Semiconductor Films for High-Performance Chemical Sensors. *Adv. Mater. Interfaces* **2016**, *3*, 1600518, 10.1002/admi.201600518.
12. Pandey, S. Highly sensitive and selective chemiresistor gas/vapor sensors based on polyaniline nanocomposite: A comprehensive review. *J. Sci. Adv. Mater. Devices* **2016**, *1*, 431-453, 10.1016/j.jsamd.2016.10.005.
13. Crowley, K.; Morrin, A.; Hernandez, A.; O'Malley, E.; Whitten, P.G.; Wallace, G.G.; Smytha, M.R.; Killard, A.J. Fabrication of an ammonia gas sensor using inkjet-printed polyaniline nanoparticles. *Talanta* **2008**, *77*, 710–717, j.talanta.2008.07.022.
14. Wannebroucq, A.; Gruntz, G.; Suisse, J.-M.; Nicolas, Y.; Meunier-Prest, R.; Mateos, M.; Toupance, T.; Bouvet, M. New n-type molecular semiconductor–doped insulator (MSDI) heterojunctions combining a

triphenodioxazine (TPDO) and the lutetium bisphthalocyanine ($LuPc_2$) for ammonia sensing. *Sens. Actuators B* **2018**, *255*, 1694–1700, 10.1016/j.snb.2017.08.184.
15. Klyamer, D.D.; Sukhih, A.S.; Krasnov, P.O.; Gromilov, S.A.; Morozova, N.B.; Basova, T.V. Thin films of tetrafluorosubstituted cobalt phthalocyanine: Structure and sensor properties. *Appl. Surf. Sci.* **2016**, *372*, 79–86, 10.1016/j.apsusc.2016.03.066.
16. Sukhikh, A.S.; Klyamer, D.D.; Parkhomenko, R.G.; Krasnov, P.O.; Gromilov, S.A.; Hassan, A.K.; Basova, T.V. Effect of fluorosubstitution on the structure of single crystals, thin films and spectral properties of palladium phthalocyanines. *Dyes Pigments* **2018**, *149*, 348–355, 10.1016/j.dyepig.2017.10.024.
17. Hesse, K.; Schlettwein, D. Spectroelectrochemical investigations on the reduction of thin films of hexadecafluorophthalocyaninatozinc ($F_{16}PcZn$). *J. Electroanal. Chem.* **1999**, *476*, 148–158, 10.1016/S0022-0728(99)00381-2.
18. Engel, M.K. Single-Crystal Structures of Phthalocyanine Complexes and Related Macrocycles. In The Porphyrin Handbook; Kadish, K.M., Smith, K.M., Guilard R., Eds.; Academic Press, USA, **2003**; v. 20, pp. 1–242; 0-12-39322.
19. Schollhorn, B.; Germain, J.P.; Pauly, A.; Maleysson, C.; Blanc, J.P. Influence of peripheral electron-withdrawing substituents on the conductivity of zinc phthalocyanine in the presence of gases. Part 1: reducing gases. *Thin Solid Films* **1998**, *326*, 245–250, 10.1016/S0040-6090(98)00553-7.
20. Ma, X.; Chen, H.; Shi, M.; Wu, G.; Wang, M.; Huang, J. High gas-sensitivity and selectivity of fluorinated zinc phthalocyanine film to some non-oxidizing gases at room temperature. *Thin Solid Films* **2005**, *489*, 257–261, 10.1016/j.tsf.2005.04.100.
21. Brinkmann, H.; Kelting, C.; Makarov, S.; Tsaryova, O.; Schnurpfeil, G.; Wöhrle, D.; Schlettwein, D. Fluorinated phthalocyanines as molecular semiconductor thin films. *Phys. Stat. Sol. (a)* **2008**, *205*, 409–420, 10.1002/pssa.200723391.
22. Becke, A.D. Density-functional exchange energy approximation with correct asymptotic behavior. *Phys. Rev. A* **1988**, *88*, 3098–3100, 10.1103/PhysRevA.38.3098.
23. Perdew, J.P. Density functional approximation for the correlation energy of the inhomogeneous electron gas. *Phys. Rev. B* **1986**, *33*, 8822–8824, 10.1103/PhysRevB.33.8822.
24. Schaefer, A.; Horn, H.; Ahlrichs, R. Fully optimized contracted Gaussian basis set for atoms Li to Kr. *J. Chem. Phys.* **1992**, *97*, 2571–2577, 10.1063/1.463096.
25. Schaefer, A.; Huber, C.; Ahlrichs, R. Fully optimized contracted Gaussian basis set of triple zeta valence quality for atoms Li to Kr. *J. Chem. Phys.* **1994**, *100*, 5829–5835, 10.1063/1.467146.
26. Grimme, S.; Ehrlich, S.; Goerigk, L. Effect of the Damping Function in Dispersion Corrected Density Functional Theory. *J. Comput. Chem.* **2011**, *32*, 1456–1465, 10.1002/jcc.21759.
27. Grimme, S.; Antony, J.; Ehrlich, S.; Krieg, H. A consistent and accurate ab initio parametrization of density functional dispersion correction (DFT-D) for the 94 elements H-Pu. *J. Chem. Phys.* **2010**, *132*, 154104, 10.1063/1.3382344.
28. Neese, F. The ORCA program system, WIREs. *Comput. Mol. Sci.* **2012**, *2*, 73-78.
29. Mulliken, R.S. Electronic Population Analysis on LCAO–MO Molecular Wave Functions. I. *J. Chem. Phys.* **1955**, *23*, 1833–1840, 10.1063/1.1740588.
30. Mulliken, R.S. Electronic Population Analysis on LCAO–MO Molecular Wave Functions. II. Overlap Populations, Bond Orders, and Covalent Bond Energies. *J. Chem. Phys.* **1955**, *23*, 1841–1846, 10.1063/1.1740589.
31. Mayer, I. Bond order and valence – relations to Mulliken population analysis. *Int. J. Quant. Chem.* **1984**, *26*, 151–154, 10.1002/qua.560260111.
32. Mayer, I. Bond orders and valences in the SCF theory – a comment. *Theor. Chim. Acta* **1985**, *67*, 315–322, 10.1007/BF00529303.
33. Liang, X.; Chen, Zh.; Wu, H.; Guo, L.; He, C.; Wang, B.; Wu, Y. Enhanced NH3-sensing behavior of 2,9,16,23-tetrakis(2,2,3,3-tetrafluoropropoxy) metal(II) phthalocyanine/multi-walled carbon nanotube hybrids: An investigation of the effects of central metals. *Carbon* **2014**, *80*, 268-278, 10.1016/j.snb.2017.10.032.
34. Tang, Q.; Li, H.; Liu, Y.; Hu, W. High-performance air-stable n-type transistors with an asymmetrical device configuration based on organic single-crystalline submicrometer/nanometer ribbons. *J. Am. Chem. Soc.* **2006**, *128*, 14634-14639, 10.1021/ja064476f.
35. Barsan, N.; Simion, C.; Heine, T.; Pokhrel, S.; Weimar, U. Modeling of sensing and transduction for p-type semiconducting metal oxide based gas sensors. *J. Electroceram.* **2010**, *25*, 11–19, 10.1007/s10832-009-9583-x.

36. Kim, H.-J; Lee, J.-H. Highly sensitive and selective gas sensors using p-type oxide semiconductors: Overview. *Sens. Actuators B* **2014**, 192, 607– 627, 10.1016/j.snb.2013.11.005.
37. Kerp, H. R.; Westerdui, K. T.; van Veen, A. T.; van Faassen, E. E. Quantification and effects of molecular oxygen and water in zinc phthalocyanine layers. *J. Mater. Res*. **2001,** *16*, 503-511, 10.1557/JMR.2001.0073.
38. de Haan, A.; Debliquy, M.; Decroly, A. Influence of atmospheric pollutants on the conductance of phthalocyanine films. *Sens. Actuators B: Chem*. **1999**, *57*, 69-74, 10.1016/S0925-4005(99)00137-9.
39. Gould R. D. Structure and electrical conduction properties of phthalocyanine thin films. *Coord. Chem. Rev.* **1996**, *156*, 237-274, 10.1016/S0010-8545(96)01238-6.
40. Schlettwein, D.; Graaf, H.; Meyer, J.-P.; Oekermann, T.; Jaeger, N.I. Molecular interactions in thin films of hexadecafluorophthalocyaninatozinc (F_{16}PcZn) as compared to islands of N,N′-dimethylperylene-3,4,9,10-biscarboximide (MePTCDI). *J. Phys. Chem. B* **1999**, *103*, 3078–3086, 10.1021/jp983111h.
41. Schlettwein, D.; Hesse, K.; Gruhn, N.E.; Lee, P.A.; Nebesny, K.W.; Armstrong, N.R. Electronic energy levels in individual molecules, thin films, and organic heterojunctions of substituted phthalocyanines. *J. Phys. Chem. B* **2001**, *105*, 4791–4800, 10.1021/jp001912q.
42. Parkhomenko, R.G.; Sukhikh, A.S.; Klyamer, D.D.; Krasnov, P.O.; Gromilov, S.A.; Kadem, B.; Hassan, A.K.; Basova, T.V. Thin films of unsubstituted and fluorinated palladium phthalocyanines: structure and sensor response toward ammonia and hydrogen. *J. Phys. Chem. C* **2017**, *121*, 1200–1209, 10.1021/acs.jpcc.6b10817.
43. Erk, P.; Hengelsberg, H.; Haddow, M.F.; van Gelder R. The innovative momentum of crystal engineering. *Cryst. Eng. Comm.* **2004**, *6*, 474–483, 10.1039/B409282A.
44. Ballirano, P.; Caminiti, R.; Ercolani, C.; Maras, A.; Orru M.A. X-ray powder diffraction structure reinvestigation of the α and β forms of cobalt phthalocyanine and kinetics of the $\alpha \rightarrow \beta$ phase transition. *J. Am. Chem. Soc.* **1998**, *120*, 12798–12807, 10.1021/ja973815p.
45. Vergnat, C.; Landais, V.; Legrand, J.-F.; Brinkmann, M. Orienting semiconducting nanocrystals on nanostructured polycarbonate substrates: impact of substrate temperature on polymorphism and in-plane orientation. *Macromolecules* **2011**, *44*, 3817–3827, 10.1021/ma200350v.
46. Pandey, P.A.; Rochford, L.A.; Keeble, D.S.; Rourke, J.P.; Jones, T.S.; Beanland, R.; Wilson N.R. Resolving the nanoscale morphology and crystallographic structure of molecular thin films: F_{16}CuPc on graphene oxide. *Chem. Mater.* **2012**, *24*, 1365–1370, 10.1021/cm300073v.
47. Yoon, S.M.; Song, H.J.; Hwang, I.-C.; Kim, K.S.; Choi H.C. Single crystal structure of copper hexadecafluorophthalocyanine (F_{16}CuPc) ribbon. *Chem. Comm.* **2010**, *46*, 231–233, 10.1039/B914457A.
48. Chen, H.-I.; Chi, C.-Y.; Chen, W.-C.; Liu, I.-P.; Chang, C.-H.; Chou, T.-C.; Liu, W.-C. Ammonia Sensing Characteristic of a Pt Nanoparticle/Aluminum-Doped Zinc Oxide Sensor. *Sens. Actuators B* **2018**, *267*, 145–154, 10.1016/j.snb.2018.04.019.
49. Wang, X.; Meng, S.; Tebyetekerwa, M.; Weng, W.; Pionteck, J.; Sun, B.; Qin, Z.; Zhu M. Nanostructured polyaniline/poly(styrene-butadiene-styrene) composite fiber for use as highly sensitive and flexible ammonia sensor. *Synth. Met.* **2017**, *233*, 86–93, 10.1016/j.synthmet.2017.09.012.
50. Matindoust, S.; Farzi, A.; Nejad, M.B.; Abadi, M.H.S.; Zou, Z.; Zheng, L.R. Ammonia gas sensor based on flexible polyaniline films for rapid detection of spoilage in protein-rich foods. *J. Mater. Sci. Mater. Electron.* **2017**, *28*, 7760–7768, 10.1007/s10854-017-6471-z.
51. Lee, K.; Scardaci, V.; Kim, H.-Y.; Hallam, T.; Nolan, H.; Bolf, B.E.; Maltbie, G.S.; Abbott, J.E.; Duesberg, G.S. Highly sensitive, transparent, and flexible gas sensors based on gold nanoparticle decorated carbon nanotubes. *Sens. Actuators B* **2013**, *188*, 571–575, 10.1016/j.snb.2013.07.048.
52. Li, X.; Wang, B.; Wang, X.; Zhou, X.; Chen, Z.; He, C.; Yu, Z.; Wu Y. Enhanced NH3-Sensitivity of Reduced Graphene Oxide Modified by Tetra-α-Iso-Pentyloxymetallophthalocyanine Derivatives. *Nanoscale Res. Lett.* **2015**, *10*, 373, 10.1186/s11671-015-1072-3.
53. Singh, A.; Kumar, A.; Kumar, A.; Samanta, S.; Joshi, N.; Balouria, V.; Debnath, A.K.; Prasad, R.; Z. Salmi, M. M. Chehimi, D.K. Aswal, S. K. Gupta, Bending stress induced improved chemiresistive gas sensing characteristics of flexible cobalt-phthalocyanine thin films. *Appl. Phys. Lett.* **2013**, *102*, 132107, 10.1063/1.4800446.